MPC based coordinated voltage regulation for distribution networks with distributed generation and energy storage system

Guo, Yifei; Wu, Qiuwei; Gao, Houlei; Chen, Xinyu; Østergaard, Jacob; Xin, Huanhai

Published in:
IEEE Transactions on Sustainable Energy

Link to article, DOI:
10.1109/TSTE.2018.2869932

Publication date:
2019

Document Version
Peer reviewed version

MPC-Based Coordinated Voltage Regulation for Distribution Networks With Distributed Generation and Energy Storage System

Yifei Guo, Qiuwei Wu, *Senior Member, IEEE,* Houlei Gao, *Member, IEEE,* Xinyu Chen, *Member, IEEE,* Jacob Østergaard, *Senior Member, IEEE*, and Huanhai Xin, *Member, IEEE*

***Abstract*—This paper presents a Model Predictive Control (MPC)-based coordinated voltage control scheme for distribution networks with high penetration of distributed generation (DG) and energy storage. In this scheme, the DG units, energy storage devices and on-load tap changer (OLTC) are optimally coordinated to maintain all bus voltages in the network within a permissable range. To better coordinate the economical operation and voltage regulation, two control modes are designed according to the operating conditions. In the preventive mode, the DG units operate in the maximum power point tracking (MPPT) mode. State-of-charge (SoC) of energy storage system (ESS) units and power outputs of DG and ESS units are optimized while maintaining the voltages within the feasible range. In the corrective mode, active power curtailment of DG units is also used as a necessary method to correct the severe voltage deviations. The voltage sensitivity coefficients with respect to the power injections and tap changes are updated in real time using an analytical sensitivity calculation method to improve the computation efficiency. A test system consisting of two 20kV feeders fed from the same substation based on a real distribution network was used to validate the proposed coordinated voltage control scheme under both normal and large-disturbance conditions.**

***Index Terms*—active power curtailment, distribution generation (DG), distribution network, energy storage, model predictive control (MPC), reactive power control, voltage control.**

I. Introduction

INTEGRATION of distributed generation (DG) into low voltage (LV)/medium voltage (MV) distribution networks is one of the most viable ways to meet the ever increased energy demand and alleviate the growing pressure over environmental issues around the world. The traditional passive distribution networks are gradually transforming into active distribution networks (ADNs) with the role of energy collection, transmission, storage and distribution [1]. DG such as photovoltaic (PV) and wind power can provide clean energy. However, with the increasing penetration of DG, it brings a number of technical challenges such as power quality, voltage regulation, protection and stability [2].

Voltage regulation issue of ADNs is one of the key issues that limits the integration of DG in networks. On one hand, DG can cause bi-directional power flow and thus create voltage rise problem on the feeders. On the other hand, the stochastic and intermittent nature of renewable energy and the high R/X ratio of LV/MV networks may lead to frequent and significant fluctuation of voltages. The distribution network operators (DNOs) cannot effectively regulate the voltage profile across the networks if only relying on the conventional voltage regulation equipments including on-load tap changer (OLTC), step voltage regulator (SVR), and switched capacitor banks (CBs), limited by their slow response, discrete actions and independent control manner [3]. To better control the voltages, more advanced control methods are urgently needed, motivating a considerable number of studies in this area.

The simplest and low-cost methods are designed in decentralized autonomous manner without any coordination between the DG units and conventional voltage control devices. The reactive power outputs or power factors of DG units are locally adjusted to mitigate the voltage rise on the feeders [4]– [7], and sometimes, the curtailment of active power of DG is inevitable to effectively regulate the voltage. The non-coordinated methods cause competition among DG units and may interface with the OLTC and SVR, posing the possibility of undesired islanding.

The centralized coordinated voltage control strategies based on optimization algorithms have been widely studied, which can achieve the optimal control performance. In such schemes, a central controller is required to collect the operating information of the whole network, solve the centralized optimization problem and send back control commands to each device. In [3], the impact of power injections of DG units on OLTC and SVR was analyzed and a voltage control strategy was

This work was supported in part by the ForskEL program through the 'IDE4L-DK Top-Up' project and in part by the China Scholarship Council (CSC).

Y. Guo is with Key Laboratory of Power System Intelligent Dispatch and Control of Ministry of Education, Shandong University, Jinan 250061, China and Center for Electric and Energy (CEE), Department of Electrical Engineering, Technical University of Denmark (DTU), Kgs. Lyngby 2800, Denmark (e-mail:yfguo.sdu@gmail.com).

Q. Wu is with the Centre for Electric Power and Energy, Department of Electrical Engineering, Technical University of Denmark, Lyngby, 2800, Denmark and the Harvard China Project, School of Engineering and Applied Sciences, Harvard University, 29 Oxford Street, Cambridge, MA 02138, USA (e-mail: qw@elektro.dtu.dk, qiuwu@seas.harvard.edu).

H. Gao is with Key Laboratory of Power System Intelligent Dispatch and Control of Ministry of Education, Shandong University, Jinan 250061, China (e-mail: houleig@sdu.edu.cn).

X. Chen is with the Harvard China Project, School of Engineering and Applied Sciences, Harvard University, 29 Oxford Street, Cambridge, MA 02138, USA (e-mail: xchen@seas.harvard.edu)

J. Østergaard is with the Center for Electric and Energy (CEE), Department of Electrical Engineering, Technical University of Denmark (DTU), Kgs. Lyngby 2800, Denmark (e-mail: joe@elektro.dtu.dk).

H. Xin is with the College of Electrical Engineering, Zhejiang University, Hangzhou 310027, China (e-mail: xinhh@zju.edu.cn).

Corresponding author: Qiuwei Wu (e-mail: qw@elektro.dtu.dk).

proposed to reduce the total number of OLTC actions over a day. In [8] and [9], the optimal power flow (OPF)-based voltage control strategies were designed, aiming to minimize the curtailed active power of DG units. A combined local and centralized active/reactive power control of PV inverters was presented in [10]. The active and reactive power of PV units are controlled by the rules based on piece-wise linear functions with tunable parameters optimized by the central controller. In [11], a coordinated voltage control strategy was proposed to allow independent power producers to offer the voltage regulation ancillary service. It was formulated into a nonlinear constrained optimization problem and solved by the sequential quadratic programming algorithm. In [12], an optimal voltage control scheme of ADNs was proposed which was formulated as a standard OPF problem and showed better control performance than the rule-based algorithm. In [13], the soft open point was also considered in voltage control and coordinated with other controllable devices including DG, CBs and OLTC. Similarly, a multi-objective mixed-integer nonlinear programming (MINLP) model for voltage control was formulated and solved using the particle swarm optimization (PSO) algorithm in [14]. In [15], a real-time demand response control scheme was proposed with the aim of continuously supporting the grid needs in terms of voltage control. In [16], the energy storage system (ESS) units were indirectly controlled by the DNOs via real-time demand response broadcast signals to provide voltage support service for the networks. In [17], a Model Predictive Control (MPC) scheme of distribution networks with PV and energy storage systems was proposed, aiming to minimize operating costs with the constraints of network voltage magnitude. In [18], a model-free centralized control strategy was proposed to regulate the active power of distributed energy resources (DERs) in LV distribution networks in order to maintain the voltages within the feasible range. In [19], both of the active and reactive power of DERs were controlled to minimize the network losses and mitigate the voltage deviations. The authors of [20] proposed a two-stage control scheme to mitigate the voltage issues caused by the solar generation by coordinating electric vehicles and conventional voltage regulation devices.

Moreover, in recent years, distributed control strategies, based on the distributed control, optimization and multi-agent techniques, have attracted a lot of attention [21]– [23]. However, to implement the distributed control scheme, several key issues must be considered firstly such as data standardization, platform, communication language, synchronization, etc [2].

The previous centralized optimization-based voltage control methods are mostly developed based on the one-step optimization models, neglecting the dynamic transition between two states. Moreover, they often have a single control mode which may be not sufficient to deal with variable operation conditions in ADNs. Moreover, the constant sensitivity coefficients obtained from the offline power flow analysis are often used, of which the errors may deteriorate the control performance.

The main contribution of this paper is a centralized coordinated voltage control scheme design based on the MPC to regulate the voltages in distribution networks with high penetration of DG and ESS. In this scheme, the active and reactive power of DG units, and charging/discharging power of ESS units are optimally coordinated. Moreover, the expected actions of OLTC are considered in the optimization problem. Compared with the existing work, the main advantages of proposed scheme are summarized as follows:

- The voltage regulation capabilities of DG units, ESS units and OLTC with different response time are fully utilized and optimally coordinated.
- The impact of OLTC actions on voltage is considered to mitigate the possible cluttering caused by the hunting between the DG/ESS units and OLTC.
- A modified clustering-based approach is proposed to better select the monitored (critical) buses in the networks.
- Two different control modes (preventive mode/corrective mode) are designed to coordinate the maximum energy usage and voltage regulation issue according to the operating conditions.

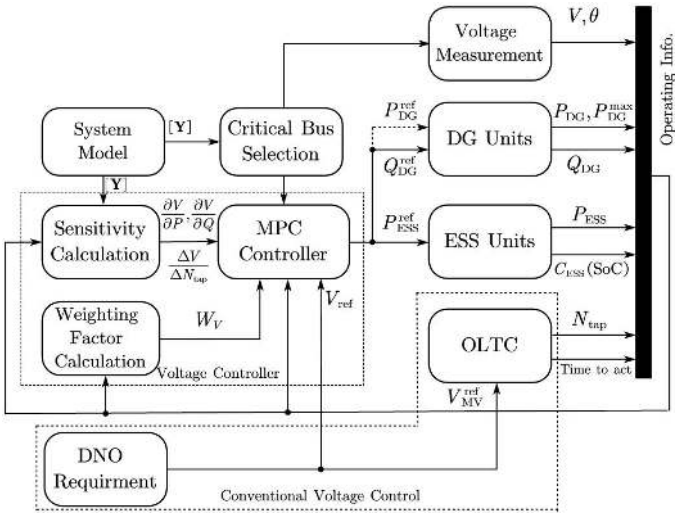

Fig. 1. Structure of the coordinated voltage control for distribution networks with DG and ESS.

The rest of this paper is organized as follows. Section II briefly introduces the proposed MPC-based coordinated voltage control scheme. Section III presents the efficient analytical sensitivity calculation method. Section IV presents the improved clustering-based method for critical bus selection. In Section V, the coordination strategy between the OLTC and MPC controller is described. In Section VI, the mathematical formulation of the MPC-based voltage control problem is presented. Section VII presents the simulation results followed by conclusions.

II. MPC-Based Coordinated Voltage Control

The centralized coordinated voltage control is performed by the DNOs by managing various controllable resources including the DG and ESS units while considering the impact of potential actions of OLTC which is controlled by its local automatic voltage control (AVC) system. The data acquisition system of the network collects the network operating information including: 1) bus voltage phasors; 2) active and reactive power injections of DG units and their maximum available

power; 3) charing/discharing power of ESS units and their SoC information; 4) operating information of OLTC transformers including the time-to-act and current tap position which can be obtained from its local AVC signals. Based on the real-time measurements, a state estimator provides the network state information to the DNOs. Next, the DNOs formulate and solve the MPC-based optimal control problem to generate the control commands of DG and ESSs. Finally, the control commands are sent to each unit. The optical fiber or WiFi communication technologies with a limited time delay can be used to achieve fast data transmission. Since the centralized control highly relies on the communication, the redundant communication network (satisfying the $N-1$ criterion) is required to guarantee the robustness of the communication network against communication failures. For computation performance, since it only requires standard QP computation with continuous variables. Various advanced commercial solvers can efficiently solve it in milliseconds.

From an economic perspective, it is costly to monitor all bus voltages in real-life implementation. Consequently, the configuration of the voltage measurement should be addressed. The clustering-based zoning method, which was originally used in secondary voltage control of transmission systems, is modified and used in this scheme to divide buses into several zones and select the critical buses of the networks, considering the effect of active power on voltages. This work can be done by offline analysis or adaptively updating in real time.

The voltage sensitivity calculation is performed to develop the linearized network model for voltage prediction. Since they vary with the operating state of the networks, an efficient analytical sensitivity calculation method is adopted to update the voltage sensitivity coefficients in each control step to guarantee the control performance.

Two control modes are designed: 1) preventive mode, which is chosen when all the monitored bus voltages are within the predefined limits; and 2) corrective mode, which is activated if any monitored bus voltage violates the limits. In the preventive mode, the DG units operate at the MPPT mode to improve the energy usage. The reactive power of DG units, and the charging/discharing power of ESS units are optimally controlled to maintain the voltages within the feasible range. Additionally, the state-of-charge (SoC) of ESS units and power output variations of DG and ESS units are optimized as well. In the corrective mode, all these devices are coordinated to correct the severe voltage deviations. The active power curtailment of DG units is also used to accelerate the voltage recovery. The potential tap changes of OLTC are predicted and considered in the MPC formulation.

The proposed MPC-based control scheme can be also applied for meshed networks. However, the sensitivity calculation method should be replaced by other methods. The sensitivity coefficients with respect to power injections can be obtained using the Jacobian matrix while those with the tap change can be calculated by the numerical method (two power flow computation with a single tap position change).

III. Sensitivity Calculation

The typical method for voltage sensitivity calculation is using the updated Jacobian matrix derived from the power flow problem. This method can only calculate the sensitivity coefficients with respect to the power injections. The Jacobian matrix needs to be rebuilt and inverted for each control period. This procedure creates non-trivial computation constraints for implementing real-time centralized or decentralized controllers. For the voltage sensitivity with respect to the tap changes, it is calculated using the numerical method: perform two runs of power flow calculation with a single tap position difference and then compare the solution. It is time-consuming and the Newton-Raphson algorithm may fail to converge due to the high R/X ratio in LV/MV distribution networks. Thus, an analytical sensitivity calculation method developed in [24] is adopted in this paper to overcome these disadvantages and improve the computation efficiency.

Suppose the network comprised of N buses including N_S slack buses and N_I buses with PQ injections. $\mathcal{S}$ and $\mathcal{I}$ denote the set of slack buses and the buses with PQ injections, respectively (i.e. $\mathcal{S}\cup\mathcal{I}=\{1,2,...,N\}$ and $\mathcal{S}\cap\mathcal{I}=\emptyset$). Define $\overline{V}_i \triangleq V_i e^{\mathrm{j}\theta_i}$ for $i\in\mathcal{S}\cup\mathcal{I}$ and $\overline{S}_i = P_i + \mathrm{j}Q_i$ for $i\in\mathcal{I}$. The relationship between bus voltages and power injections is,

$$\underline{S}_i = \underline{V}_i \sum_{j\in\mathcal{S}\cup\mathcal{I}} \overline{Y}_{\mathrm{bus},ij}\overline{V}_j \tag{1}$$

where $\overline{Y}_{\mathrm{bus},ij}$ denotes the elements of the admittance matrix $[\overline{Y}_{\mathrm{bus}}]_{N\times N}$. $\underline{S}_i$ and $\underline{V}_i$ denote the conjugates of $\overline{S}_i$ and $\overline{V}_i$, respectively. The following sensitivity calculation is based on this equation.

A. Voltage Sensitivity With Respect to Power Injections

Firstly, the partial derivatives of $\underline{S}_i$ for $i\in\mathcal{I}$ with respect to active power injection P_l and reactive power injection Q_l of a bus $l\in\mathcal{I}$ should be calculated, which satisfy the following equations,

$$\begin{aligned}\frac{\partial\underline{S}_i}{\partial P_l} =& \frac{\partial\left\{P_i-\mathrm{j}Q_i\right\}}{\partial P_l} = \frac{\partial\underline{V}_i}{\partial P_l}\sum_{j\in\mathcal{S}\cup\mathcal{I}}\overline{Y}_{\mathrm{bus,ij}}\overline{V}_j \\ &+\underline{V}_i\sum_{j\in\mathcal{I}}\overline{Y}_{\mathrm{bus},ij}\frac{\partial\overline{V}_j}{\partial P_l} = \begin{cases}1, & \text{for } i=l.\\ 0, & \text{for } i\neq l.\end{cases}\end{aligned} \tag{2}$$

$$\begin{aligned}\frac{\partial\underline{S}_i}{\partial Q_l} =& \frac{\partial\left\{P_i-\mathrm{j}Q_i\right\}}{\partial Q_l} = \frac{\partial\underline{V}_i}{\partial Q_l}\sum_{j\in\mathcal{S}\cup\mathcal{I}}\overline{Y}_{\mathrm{bus},ij}\overline{V}_j \\ &+\underline{V}_i\sum_{j\in\mathcal{I}}\overline{Y}_{\mathrm{bus},ij}\frac{\partial\overline{V}_j}{\partial Q_l} = \begin{cases}-\mathrm{j}1, & \text{for } i=l.\\ 0, & \text{for } i\neq l.\end{cases}\end{aligned} \tag{3}$$

It can be observed that (2) is linear with respect to $\partial\overline{V}_i/\partial P_l$ and $\partial\underline{V}_i/\partial P_l$; and (3) is linear with respect to $\partial\overline{V}_i/\partial Q_l$ and $\partial\underline{V}_i/\partial Q_l$. Thus, once $\partial\overline{V}_i/\partial P_l$, $\partial\underline{V}_i/\partial P_l$, $\partial\overline{V}_i/\partial Q_l$ and $\partial\underline{V}_i/\partial Q_l$ are obtained, the voltage sensitivity coefficients with respect to power injections can be calculated by,

$$\frac{\partial V_i}{\partial P_l} = \frac{1}{V_i}\mathrm{Re}\left(\underline{V}_i\frac{\partial\overline{V}_i}{\partial P_l}\right) \tag{4}$$

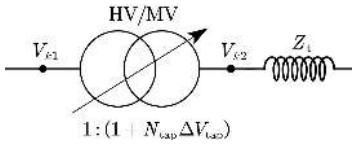

Fig. 2. Equivalent model of an OLTC transformer.

$$\frac{\partial V_i}{\partial Q_l} = \frac{1}{V_i}\mathrm{Re}\left(\underline{V}_i \frac{\partial \overline{V}_i}{\partial Q_l}\right) \tag{5}$$

B. Voltage Sensitivity With Respect to Tap Changes

It is assumed that the OLTC transformer is located at the slack bus of the distribution network. Since it is difficult to directly calculate the voltage sensitivity coefficients with respect to tap changes, the voltage sensitivity coefficients with respect to the slack bus voltage are derived firstly and then the voltage sensitivity coefficients with respect to tap changes can be obtained. For a bus $i \in \mathcal{I}$, the partial derivatives with respect to voltage magnitude V_k of a slack bus $k \in \mathcal{S}$ are derived by,

$$-\overline{V}_i \overline{Y}_{\mathrm{bus},ik} e^{\mathrm{j}\theta_k} = \underline{W}_{ik} \sum_{j \in \mathcal{S}\cup\mathcal{I}} \overline{Y}_{\mathrm{bus},ij}\overline{V}_j + \underline{V}_i \sum_{j\in\mathcal{I}} \overline{Y}_{\mathrm{bus},ij}\overline{W}_{jk} \tag{6}$$

where

$$\overline{W}_{ik} = \frac{\partial \overline{V}_i}{\partial V_k} = \left(\frac{1}{V_i}\frac{\partial V_i}{\partial V_k} + \mathrm{j}\frac{\partial \theta_i}{V_k}\right)\overline{V}_i.$$

Similarly, (6) is linear with respect to $\overline{W}_{ik}$ and $\underline{W}_{ik}$. Once $\overline{W}_{ik}$ and $\underline{W}_{ik}$ are obtained, the sensitivity coefficients with respect to the slack bus voltage magnitude at bus $k \in \mathcal{S}$ can be calculated by,

$$\frac{\partial V_i}{\partial V_k} = V_i \mathrm{Re}\left(\frac{\overline{W}_{ik}}{\overline{V}_i}\right). \tag{7}$$

Considering a transformer with OLTC on the secondary winding (MV side) as illustrated in Fig. 2, the ratio relationship can be expressed as,

$$\frac{V_{k2}}{V_{k1}} = (1 + N_{\mathrm{tap}} \cdot \Delta V_{\mathrm{tap}}) \cdot \frac{V_{N1}}{V_{N2}} \tag{8}$$

where V_{k1} and V_{k2} are the primary and secondary voltage of the ideal transformer, respectively; V_{N1} and V_{N2} are the nominal voltages of the transformer, N_{tap} is the tap position and ΔV_{tap} is the voltage step per tap; Z_t is the equivalent impedance of the transformer. Suppose the slack bus voltage V_{k1} keeps constant and the tap position moves from N_{tap} to N'_{tap} ($\Delta N_{\mathrm{tap}} = N'_{\mathrm{tap}} - N_{\mathrm{tap}}$), the sensitivity coefficient of V_{k2} with respect to the tap change N_{tap} can be obtained by,

$$\frac{\Delta V_{k2}}{\Delta N_{\mathrm{tap}}} = V_{k1} \cdot \Delta V_{\mathrm{tap}} \cdot \frac{V_{N1}}{V_{N2}}. \tag{9}$$

Then, combining (7) and (9), the voltage sensitivity coefficients with respect to tap changes can be calculated by,

$$\frac{\Delta V_i}{\Delta N_{\mathrm{tap}}} = V_{k1} \cdot \Delta V_{\mathrm{tap}} \cdot \frac{V_{N1}}{V_{N2}} \cdot \frac{\partial V_i}{\partial V_k}. \tag{10}$$

IV. Critical Bus Selection

To regulate the voltages of the distribution networks within the permissable range, the controller should know the real-time operating states of the distribution networks. However, the complete supervisor control and data acquisition (SCADA) system is impractical in distribution networks considering the heavy burden of investment, implying that it is impossible to monitor all bus voltages in the networks. Therefore, several representative critical buses, which can reflect the whole system operating conditions, should be selected as the monitored buses. Thus, a systematic critical bus selection method based on the clustering technique is proposed in this paper, by modifying the zoning method in the secondary voltage control of transmission systems.

The concept of electrical distance was first introduced in [25], which is calculated only using the sensitivity coefficients $\partial V/\partial Q$. The coupling between two buses is quantified by $\alpha_{ij} = (\partial V_i/\partial Q_j)/(\partial V_j/\partial Q_j)$. This is based on the assumption that the voltage variations are decoupled with the active power injections due to the low R/X ratio. In the LV/MV distribution networks, the impact of active power injections should be taken into account. The sum of the voltage sensitivity coefficients with respect to active and reactive injections is considered to represent the comprehensive sensitivity. Therefore, the degree of coupling in terms of voltage between buses i and j is quantified by,

$$\alpha_{ij} = \frac{|\frac{\partial V_i}{\partial P_j}| + |\frac{\partial V_i}{\partial Q_j}|}{|\frac{\partial V_j}{\partial P_j}| + |\frac{\partial V_j}{\partial Q_j}|}. \tag{11}$$

Then, the electrical distance between buses i and j can be defined as [25],

$$D_{ij} = -\log(\alpha_{ij} \cdot \alpha_{ji}). \tag{12}$$

There are several commonly used clustering methods such as the hierarchical clustering method, k-means algorithm, fuzzy-c means algorithm and spectral-way clustering method [26]– [27]. In this paper, the hierarchical clustering method (agglomerative clustering) is used to divided the buses into several groups. In the beginning, each bus represents a cluster. Then, the distance between two clusters C_I and C_J is computed by,

$$D_{IJ} = \min\{D_{ij} : i \in C_I \text{ and } j \in C_J\}. \tag{13}$$

Then, the clusters are merged based on,

$$C_I \cup C_J : \min\{D_{IJ}\}. \tag{14}$$

The steps are carried out iteratively to form a dendrogram. Finally, a threshold is chosen to determine the zoning results.

After that, for each zone, the critical buses can be determined by the following principle: since all DG-connected buses are monitored, if the group includes the DG-connected buses, these connected buses will be selected as the critical buses; otherwise, the buses at the end of feeder are first considered to be selected. For sensitivity coefficients updating using the method developed in Section III, all the critical bus voltages can be directly obtained (measured) and the other non-critical bus voltages are assumed to be equal to the critical

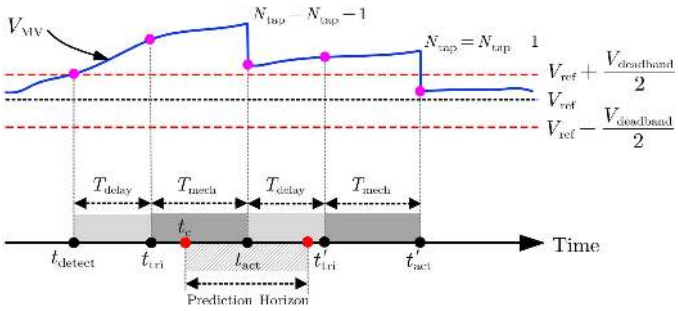

Fig. 3. The principle of OLTC operation.

bus voltages with the small electrical distance. It is expected that the closed-loop nature of MPC will compensate the minor errors of sensitivity coefficients.

V. Coordination With OLTC

The OLTC is an efficient voltage control device which can directly change the voltage level of the whole networks. In general, the OLTC is controlled only using the local automatic voltage regulator. The principle of OLTC operation is illustrated in Fig. 3.

The OLTC will perform a tap change if the controlled bus voltage (The voltage of the MV side bus of the main substation transformer V_{MV} is controlled by the OLTC.) violates the predefined dead-band V_{deadband} for longer than a predefine time delay T_{delay}, i.e.,

$$\Delta N_{\mathrm{tap}} = \begin{cases} +1, & \text{if } V_{\mathrm{MV}} < V_{\mathrm{MV}}^{\mathrm{ref}} - \dfrac{V_{\mathrm{deadband}}}{2} \\ -1, & \text{if } V_{\mathrm{MV}} > V_{\mathrm{MV}}^{\mathrm{ref}} + \dfrac{V_{\mathrm{deadband}}}{2} \end{cases} \tag{15}$$

where V_{deadband} and T_{delay} are introduced in order to avoid frequent and unnecessary switching around the reference voltage $V_{\mathrm{MV}}^{\mathrm{ref}}$, which may reduce OLTC lifetime. V_{deadband} is often designed symmetrical around the reference. The mechanical time delay T_{mech}, typically in $3-10$ s, is required for the OLTC to move the taps by one position. The non-sequential mode is adopted for the OLTC, in which the OLTC makes no distinction between the first and subsequent tap changes. Thus, suppose the tap action is triggered at $t = t_{\mathrm{tri}}$, the time of the tap change can be estimated as $t_{\mathrm{act}} = t_{\mathrm{tri}} + T_{\mathrm{mech}}$.

At each control point, if the tap action has been triggered and the current tap position is not at the minimum $\underline{N}_{\mathrm{tap}}$ or maximum position $\overline{N}_{\mathrm{tap}}$, the triggered time t_{tri} and current tap position N_{tap} will be sent to the voltage controller (if not, the "No Action" signal will be sent). Then the voltage controller will detect if there is a potential tap change within the prediction horizon H_p. Suppose the control period is T_c, the number of prediction steps is N_p ($N_p = H_p/T_c$) and the current time is t_0, the indication of the potential tap change for the kth prediction step $\mathrm{Sign}_{\mathrm{tap}}[k]$ can be obtained by,

$$\mathrm{Sign}_{\mathrm{tap}}[k] = \begin{cases} 1, & \text{if } t_{\mathrm{act}} \le t_0 + k \times T_c \\ & \text{and } \underline{N}_{\mathrm{tap}} < N_{\mathrm{tap}} < \overline{N}_{\mathrm{tap}}. \\ 0, & \text{otherwise.} \end{cases} \tag{16}$$

Compared with those optimization methods in which the OLTC is directly included in the optimization model as a control variable, the proposed coordination method has the following advantages: 1) It just needs time information sent from the OLTC controller rather than changing the existing control structure of OLTC, implying low extra investment and better feasibility; 2) It could avoid the heavy computation burden of the formulated MINLP problem due to the introduction of discrete control variables.

VI. MPC Formulation of the Coordinated Voltage Control Scheme

In the MPC, the control commands are obtained by solving a discrete-time optimal control problem over a given horizon H_p. An optimal control command sequence is produced and only the first control in the sequence is applied. The control period T_c is normally designed in seconds. From the computation perspective, the length of prediction steps N_p and control steps N_c should be equal. In this following subsections, the MPC formulation of the proposed coordinated voltage control scheme including two control modes is developed.

A. Modelling

1) DG units: The inverter-based DG is considered in this paper. Since the control period is designed in seconds, which is much longer than the response time of voltage source converter (VSC)-based inverter (in milliseconds), the dynamics of power reference tracking of the inverter can be neglected, i.e., $P_{\mathrm{DG}} = P_{\mathrm{DG}}^{\mathrm{ref}}$ and $Q_{\mathrm{DG}} = Q_{\mathrm{DG}}^{\mathrm{ref}}$, with the power output and rate limits,

$$0 \le P_{\mathrm{DG}} \le P_{\mathrm{DG}}^{\max}, \tag{17}$$

$$|\Delta P_{\mathrm{DG}}| < \Delta P_{\mathrm{DG}}^{\max}, \tag{18}$$

$$\sqrt{P_{\mathrm{DG}}^2 + Q_{\mathrm{DG}}^2} \le S_{\mathrm{DG}}, \tag{19}$$

$$|\Delta Q_{\mathrm{DG}}| \le \Delta Q_{\mathrm{DG}}^{\max}. \tag{20}$$

where P_{DG}, Q_{DG}, and S_{DG} are the active, reactive power and nominal capacity of DG units; $P_{\mathrm{DG}}^{\max}$ is the maximum available power; $\Delta P_{\mathrm{DG}}^{\max}$ and $\Delta Q_{\mathrm{DG}}^{\max}$ denote the power rate limits. For the constraint (19), if active and reactive are both optimized, a solution with decoupled constraint is performed first and then if they exceeds the capacity limit, a proportional scale method is used to fulfill the constraint. If only reactive power is controlled, its limit is calculated based on the current active power.

2) ESS units: The ESS unit can be modeled by a simple integrator and its SoC in discrete time can be described by,

$$C_{\mathrm{ESS}}[k+1] = C_{\mathrm{ESS}}[k] - P_{\mathrm{ESS}}[k] \cdot \Delta t - \eta_{\mathrm{loss}} \cdot C_{\mathrm{ESS}}[k] \tag{21}$$

with the operation limits,

$$C_{\mathrm{ESS}}^{\min} \le C_{\mathrm{ESS}} \le C_{\mathrm{ESS}}^{\max}, \tag{22}$$

$$P_{\mathrm{ESS}}^{\min} \le P_{\mathrm{ESS}} \le P_{\mathrm{ESS}}^{\max}, \tag{23}$$

$$|\Delta P_{\mathrm{ESS}}| \le \Delta P_{\mathrm{ESS}}^{\max}, \tag{24}$$

where C_{ESS} denotes the charging quantity (SoC $= C_{\mathrm{ESS}}/C_{\mathrm{ESS}}^{\max}$), P_{ESS} denotes the discharging power and η_{loss} denotes the loss coefficients. Since the time scale of the studied

problem in this paper is in the range of seconds to minutes, the loss term can be neglected. $P_{\rm ESS}^{\min}$ and $P_{\rm ESS}^{\max}$ denote the power output limits. $\Delta P_{\rm ESS}^{\max}$ denotes the power rate limit.

3) Network: Generally, the distribution networks can be modeled by the power flow equations. In this paper, a linearized model derived from the Taylor approximation at the operating point is used to predict the voltage $\hat{V}$ affected by the control variables, which is,

$$\hat{V} = V[0] + \frac{\partial V}{\partial P^\top}\Delta P + \frac{\partial V}{\partial Q^\top}\Delta Q + \frac{\Delta V}{\Delta N_{\rm tap}}\Delta N_{\rm tap}. \quad (25)$$

where $V[0]$ denote the current voltage; ΔP, ΔQ and $\Delta N_{\rm tap}$ denote the variations of active/reactive power injections and tap position, respectively.

B. MPC Formulation

Firstly, the incremental vectors of $P_{\rm DG}$, $Q_{\rm DG}$, $P_{\rm ESS}$, and the vector of SoC are defined as,

$$\begin{aligned}
\Delta P_{\rm DG}[k] &\triangleq [\Delta P_{{\rm DG}_1}[k], \Delta P_{{\rm DG}_2}[k], \ldots, \Delta P_{{\rm DG}_{N_{\rm DG}}}[k]]^\top,\\
\Delta Q_{\rm DG}[k] &\triangleq [\Delta Q_{{\rm DG}_1}[k], \Delta Q_{{\rm DG}_2}[k], \ldots, \Delta Q_{{\rm DG}_{N_{\rm DG}}}[k]]^\top,\\
\Delta P_{\rm ESS}[k] &\triangleq [\Delta P_{{\rm ESS}_1}[k], \Delta P_{{\rm ESS}_2}[k], \ldots, \Delta P_{{\rm ESS}_{N_{\rm ESS}}}[k]]^\top,\\
{\rm SoC}[k] &\triangleq [{\rm SoC}_1[k], {\rm SoC}_2[k], \ldots, {\rm SoC}_{N_{\rm ESS}}[k]]^\top,
\end{aligned}$$

where $\Delta P_{{\rm DG}_i}[k] \triangleq P_{{\rm DG}_i}[k] - P_{{\rm DG}_i}[0]$, $\Delta Q_{{\rm DG}_i}[k] \triangleq Q_{{\rm DG}_i}[k] - Q_{{\rm DG}_i}[0]$, $\Delta P_{{\rm ESS}_i}[k] \triangleq P_{{\rm ESS}_i}[k] - P_{{\rm ESS}_i}[0]$. $P_{{\rm DG}_i}[0]$, $Q_{{\rm DG}_i}[0]$, and $P_{{\rm ESS}_i}[0]$ are their current values.

1) Preventive mode: If all the monitored buses including the MV side bus of main substation are within the predefined limit, i.e., $\|V_{\rm cri} - V_{\rm ref}\| < V_{\rm cri}^{\rm th}$, the MPC controller will be in the preventive control mode where $V_{\rm cri}^{\rm th}$ is the threshold value. For $V_{\rm MV}$, the threshold is $V_{\rm deadband}/2$, which is typically twice the tap step, and, for other buses, it is typically 0.05 p.u.$\sim$$0.1$ p.u.. $V_{\rm ref}$ is the reference value derived from system operators (typically 1.0 p.u.). The voltage vector of M critical buses is defined as $V_{\rm cri} \triangleq [V_{{\rm cri}_1}, V_{{\rm cri}_2}, ..., V_{{\rm cri}_M}]^\top$. In the preventive mode, DG units operates in the MPPT mode to capture more energy. The control variables are the the reactive power outputs of DG units $Q_{\rm DG}$ and charging/discharing power of ESS units $P_{\rm ESS}$. The voltages, power output variations of DG and ESS units are optimized. Besides, the SoC of ESS unit will be included in the cost function if it violates the predefined limits $[{\rm SoC}_{\rm mid} - \varepsilon, {\rm SoC}_{\rm mid} + \varepsilon]$ where ${\rm SoC}_{\rm mid}$ is typically 50%. The mathematical model of the MPC problem can be formulated as,

$$\begin{aligned}
\min \sum_{k=1}^{N_p} \Big(& \left\| \hat{V}_{\rm cri}[k] - V_{\rm ref} \right\|_{W_{\rm V}}^2 + \|{\rm SoC}[k] - {\rm SoC}_{\rm mid}\|_{W_{\rm SoC}}^2 \\
& + \|\Delta Q_{\rm DG}[k] - \Delta Q_{\rm DG}[k-1]\|_{W_{\Delta{\rm DG}}}^2 \\
& + \|\Delta P_{\rm ESS}[k] - \Delta P_{\rm ESS}[k-1]\|_{W_{\Delta{\rm ESS}}}^2 \Big) \quad (26)
\end{aligned}$$

subject to

$$Q_{{\rm DG}_i}^{\min} \le Q_{{\rm DG}_i}[0] + \Delta Q_{{\rm DG}_i}[k] \le Q_{{\rm DG}_i}^{\max},\ \forall i, \forall k \quad (27)$$

$$P_{{\rm ESS}_i}^{\min} \le P_{{\rm ESS}_i}[0] + \Delta P_{{\rm ESS}_i}[k] \le P_{{\rm ESS}_i}^{\max},\ \forall i, \forall k \quad (28)$$

$$-\Delta Q_{{\rm DG}_i}^{\max} \le \Delta Q_{{\rm DG}_i}[k] - \Delta Q_{{\rm DG}_i}[k-1] \le \Delta Q_{{\rm DG}_i}^{\max},\ \forall i, \forall k \quad (29)$$

$$-\Delta P_{{\rm ESS}_i}^{\max} \le \Delta P_{{\rm ESS}_i}[k] - \Delta P_{{\rm ESS}_i}[k-1] \le \Delta P_{{\rm ESS}_i}^{\max},\ \forall i, \forall k \quad (30)$$

$${\rm SoC}_i^{\min} \le {\rm SoC}_i[k] \le {\rm SoC}_i^{\max},\ \forall i, \forall k \quad (31)$$

$${\rm SoC}_i[k] = {\rm SoC}_i[k-1] - P_{{\rm ESS}_i}[k-1] \cdot T_c / C_{{\rm ESS}_i}^{\max},\ \forall i, \forall k \quad (32)$$

$$\hat{V}_{{\rm cri}_i}[k] = V_{{\rm cri}_i}[0] + \frac{\partial V_{{\rm cri}_i}}{\partial Q_{\rm DG}^\top} \cdot \Delta Q_{\rm DG}[k] + \frac{\partial V_{{\rm cri}_i}}{\partial P_{\rm ESS}^\top} \cdot \Delta P_{\rm ESS}[k] \quad \forall i, \forall k \quad (33)$$

where $W_{\rm V}$, $W_{\rm SoC}$, $W_{\Delta{\rm DG}}$, and $W_{\Delta{\rm ESS}}$ are the diagonal weighting matrixes for voltages, SoC, power output variations of DG and ESS units. The vector of the predicted critical bus voltages is defined as $\hat{V}_{\rm cri}[k] \triangleq [\hat{V}_{{\rm cri}_1}[k], \hat{V}_{{\rm cri}_2}[k]], \ldots, \hat{V}_{{\rm cri}_M}[k]]^\top$.

2) Corrective mode: If any monitored bus violates the limits, the MPC controller will be switched to the corrective mode to correct the voltages. In addition to $Q_{\rm DG}$ and $P_{\rm ESS}$, the active power outputs of DG units $P_{\rm DG}$ are also controlled to help the voltage correction. The voltage deviations and curtailed energy are minimized in this mode. The mathematical model can be formulated as,

$$\min \sum_{k=1}^{N_p} \left(\left\| \hat{V}_{\rm cri}[k] - V_{\rm ref} \right\|_{W_{\rm V}}^2 + \|P_{\rm DG}[k] - P_{\rm DG}^{\max}[k]\|_{W_{\rm E}}^2 \right) \quad (34)$$

subject to

$$0 \le P_{{\rm DG}_i}[0] + \Delta P_{{\rm DG}_i}[k] \le P_{{\rm DG}_i}^{\max},\ \forall i, \forall k \quad (35)$$

$$Q_{{\rm DG}_i}^{\min} \le Q_{{\rm DG}_i}[0] + \Delta Q_{{\rm DG}_i}[k] \le Q_{{\rm DG}_i}^{\max},\ \forall i, \forall k \quad (36)$$

$$P_{{\rm ESS}_i}^{\min} \le P_{{\rm ESS}_i}[0] + \Delta P_{{\rm ESS}_i}[k] \le P_{{\rm ESS}_i}^{\max},\ \forall i, \forall k \quad (37)$$

$$-\Delta Q_{{\rm DG}_i}^{\max} \le \Delta Q_{{\rm DG}_i}[k] - \Delta Q_{{\rm DG}_i}[k-1] \le \Delta Q_{{\rm DG}_i}^{\max},\ \forall i, \forall k \quad (38)$$

$$-\Delta P_{{\rm ESS}_i}^{\max} \le \Delta P_{{\rm ESS}_i}[k] - \Delta P_{{\rm ESS}_i}[k-1] \le \Delta P_{{\rm ESS}_i}^{\max},\ \forall i, \forall k \quad (39)$$

$${\rm SoC}_i^{\min} \le {\rm SoC}_i[k] \le {\rm SoC}_i^{\max},\ \forall i, \forall k \quad (40)$$

$${\rm SoC}_i[k] = {\rm SoC}_i[k-1] - P_{{\rm ESS}_i}[k-1] \cdot T_c / C_{{\rm ESS}_i}^{\max},\ \forall i, \forall k \quad (41)$$

$$\hat{V}_{{\rm cri}_i}[k] = V_{{\rm cri}_i}[0] + \frac{\partial V_{{\rm cri}_i}}{\partial P_{\rm DG}^\top} \cdot \Delta P_{\rm DG}[k] + \frac{\partial V_{{\rm cri}_i}}{\partial Q_{\rm DG}^\top} \cdot \Delta Q_{\rm DG}[k] + \frac{\partial V_{{\rm cri}_i}}{\partial P_{\rm ESS}^\top} \cdot \Delta P_{{\rm ESS}_i}[k] + {\rm Sign}_{\rm tap}[k] \cdot \frac{\Delta V_{\rm cri}}{\Delta N_{\rm tap}} \cdot \Delta N_{\rm tap},\ \forall i, \forall k \quad (42)$$

where $W_{\rm V}$ and $W_{\rm E}$ are the diagonal weighting matrixes for voltage and energy curtailment, respectively. To better correct the severe voltage deviations, for $W_{\rm V}$, the elements are determined by a dynamic weighting allocation method [28].

The presented MPC problem can be transformed into a standard quadratic programming (QP) problem and efficiently solved by the commercial QP solvers in milliseconds.

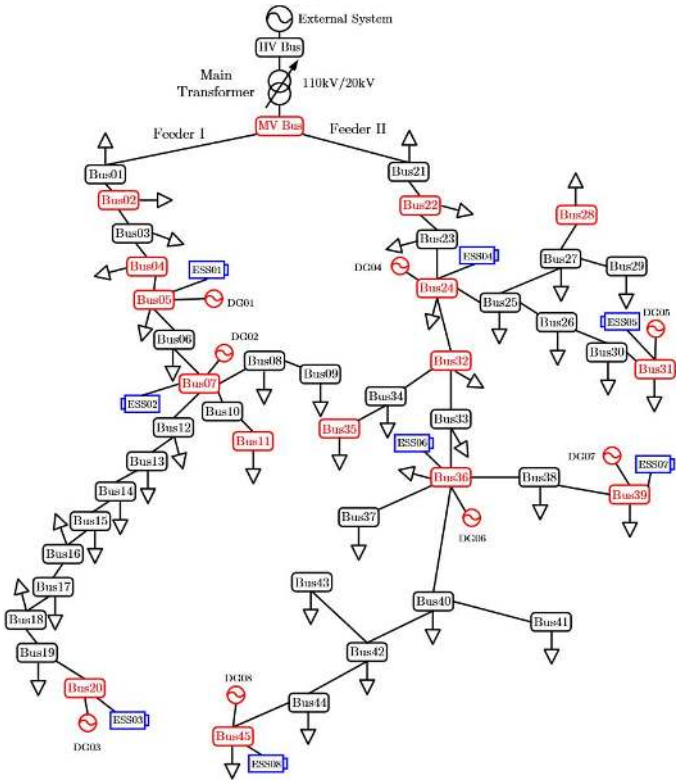

Fig. 4. The network topology.

TABLE I
PARAMETERS OF DG AND ESS UNITS

DG No.	Location	Capacity(MW)	ESS Capacity(MWh)
DG 01	Bus05	0.5	0.1
DG 02	Bus07	2	0.4
DG 03	Bus20	2	0.4
DG 04	Bus24	0.5	0.1
DG 05	Bus31	0.5	0.1
DG 06	Bus36	0.5	0.1
DG 07	Bus39	2	0.4
DG 08	Bus45	0.5	0.1

VII. CASE STUDY

In this section, the performance of the proposed MPC-based coordinated voltage control scheme is tested in a modified Finnish distribution network consisting of two 20 kV feeders, of which the network topology is presented in Fig. 4. More details of network parameters can be found in [12]. Eight DG units are connected to the network. Each DG unit is equipped with an ESS unit. The detailed information of the DG and ESS units is listed in Table I. The automatic voltage control relay of the substation and tap changing mechanism is included in the simulation. The predefined deadband V_{deadband} and time delay T_{delay} are set as 4% and $3\,\text{s}$. The tap changing range of OLTC is $\pm 9 \times 1.67\%$ and the mechanical delay is $5\,\text{s}$. The test system with the proposed controller is simulated in Matlab/SIMULINK. The controller is implemented using a MATLAB-function block with a packaging triggered subsystem. The data latency is set as 150 ms in the simulation.

The control period T_c, control horizon H_c and prediction horizon H_p of the MPC are designed as 2 s, 10 s, and 10 s, respectively (i.e., $N_p = N_c = 5$). The deadband of the SoC ε is set as 10%. Two operation scenarios are considered in the simulation. Firstly, the control performance under normal operation only considering the fluctuation of DG power outputs and network load is tested. Secondly, the operation with large disturbances induced by the external grid is considered.

TABLE II
ZONING AND CRITICAL BUS SELECTION (IN BOLD)

No.	Buses	No.	Buses
1	**01**	9	**24**
2	**02**, 03	10	25, 26, 27, 29, 30, **31**
3	**04**	11	**28**
4	**05**, 06, **07**, 08, 09, 12, 13	12	32
5	10, **11**	13	33, **36**, 37, 38, 40, 41,
6	14, 15, 16, 17, 18, 19, **20**		42, 43, 44, **45**
7	**21**	14	34, **35**
8	**22**, 23	15	**39**

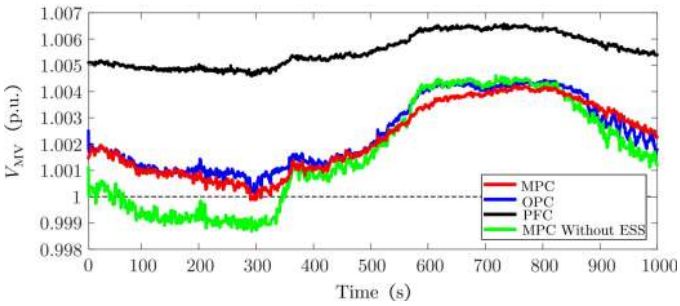

Fig. 5. Voltage of MV side bus of the main transformer.

The zoning and critical bus selection results by selecting the threshold of 0.1, are listed in Table II (critical buses in bold).

A. Normal Operation

In this subsection, the control performance of the MPC-based coordinated voltage control method under normal operation is examined and compared with the conventional local power factor control (PFC) and the one-step optimization-based optimal control (OPC). For the local PFC control, each DG unit operates with constant power factor, i.e., $Q = P \tan\varphi$ where φ is the power factor angle. To prevent the overvoltage issue, all DG units operate with the constant lagging power factor and $\cos\varphi = 0.95$ is considered in this study. For the OPC, the control period is also set as 2 s and it also has two same control modes with the MPC. Moreover, to illustrate the impact of the ESS in voltage regulation problem, the results of MPC without ESS are obtained for a comparison. The total simulation time is 1000 s. The simulation results are shown in Figs. 5 $\sim$ 7.

As shown in Fig. 5 and 6, the MPC and OPC can both effectively regulate the voltages with small deviations and fluctuations. The fluctuation is mainly caused by the active power variations of DG units. Comparatively, the MPC performs better than the OPC. The PFC fails to regulate the voltage at the end of the feeder (V_{Bus20}) within the feasible range. Moreover, introducing the ESS into voltage regulation

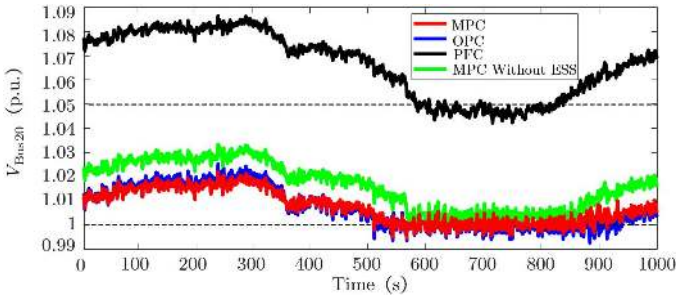

Fig. 6. Voltage of Bus20.

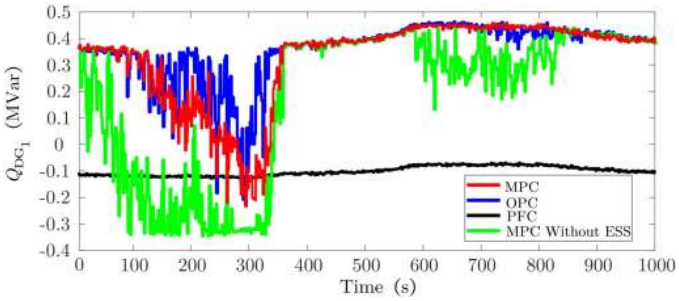

Fig. 7. Reactive power output of DG01.

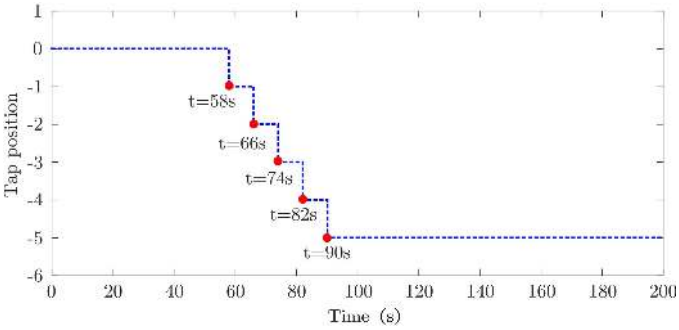

Fig. 8. Tap position.

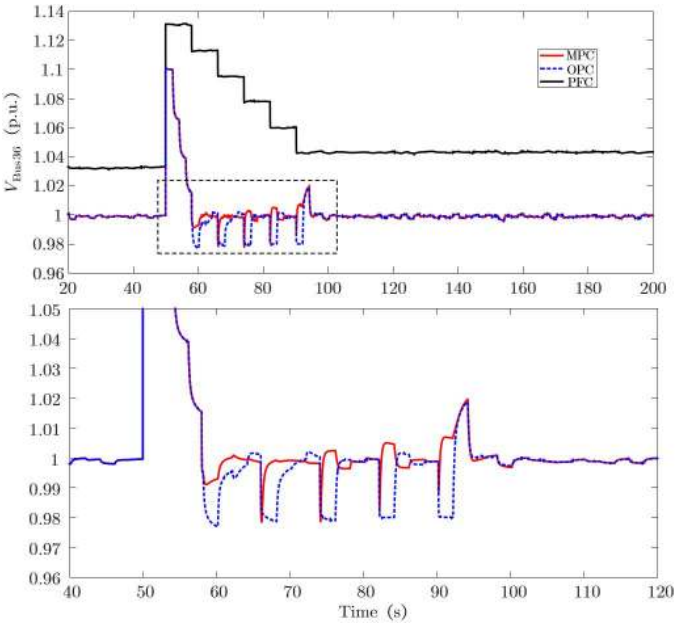

Fig. 9. Voltage of Bus36.

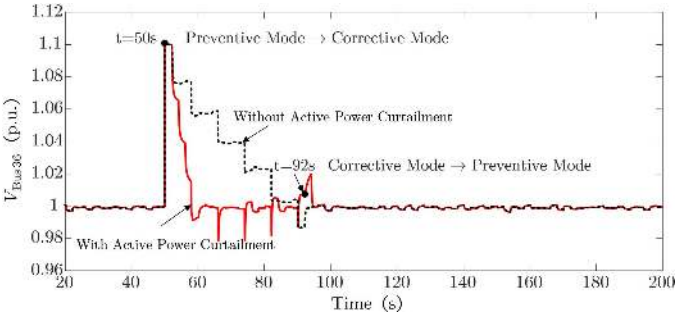

Fig. 10. Voltage of Bus36 under MPC with/without active power curtailment.

can better regulate the voltages with smaller deviations and fluctuations.

It can be seen from Fig. 7, compared with other methods, the MPC can better smooth the reactive power outputs of DG units. If the ESS is not included, the reactive power outputs of DG units may reach their limits, which may cause inadequate reactive power reserve under large-disturbance conditions. In other words, the ESS can alleviate the reactive power burdens of DG units.

B. Operation With Large Disturbance

In this subsection, to demonstrate the control performance during large-disturbance conditions, the network is affected by a large disturbance in the external grid, namely a sudden voltage increase of 0.1 p.u. at the slack bus ($t = 50$ s), which causes all bus voltages increase in the distribution network. Fig. 8 shows the tap changes of the OLTC transformer. Fig. 9 shows the voltage at Bus36. As can be seen, both of the OPC and MPC can better recover the voltage. Compared with the OPC, the MPC can make the voltage recover much faster and smoother due to the prediction mechanism and better coordination with the OLTC. The PFC shows limited voltage control capability.

The coordination between the OLTC (discrete and slow response) and DG/ESS units (continuous and fast response capability) can be explained as follows. For instance, at the control point of $t = 74$ s, since the DNO knows that there will be a tap change occuring at $t = 74$ s (actually, the tap action signal is triggered at $t = 69$ s but there is a mechanic time delay of 5 s), the DNO considers the potential tap change when optimizing the outputs of DG and ESS units. Thus, from Fig. 9, it can be observed that, after the tap change at $t = 74$ s, the voltage fast recovers close to 1.0 p.u..

To further illustrate the impact of active power curtailment of DG units on voltage regulation, the simulation results of the MPC with and without considering active power curtailment are compared. As can be seen from Fig. 10, the voltage at Bus36 recovers much faster and smoother when considering the necessary active power curtailment of DG units, implying that the active power curtailment can significantly improve the voltage regulation capability during the large-disturbance conditions. There are sudden voltage fluctuations from $t = 92$

s to $t = 94$ s when considering the active power curtailment. It is because at $t = 92$ s the controller detects the voltages have recovered within the feasible range and thus the controller switches from the corrective mode to the preventive mode where the control objectives are different.

VIII. Conclusion

This paper presents a MPC-based coordinated voltage control scheme for distribution networks with high penetration of DG and ESS. The proposed controller optimally coordinates power outputs of DG units, ESS units and the tap position of OLTC to regulate the voltages within the feasible range. Two control modes are designed for the normal operation and the operation with large voltage disturbances, respectively. The simulation results show that the proposed controller is able to maintain the voltages within the predefined range during the normal condition and accelerate and smoothen the voltage recovery during the large-disturbance conditions. Compared with the conventional PFC and OPC, the MPC shows better control performances. Moreover, the participation of ESS and necessary active power curtailment of DG units can significantly improve the voltage regulation capability especially under large disturbances.

Since LV distribution networks are often unbalanced with three-phase four wires, the proposed voltage control scheme will be extended to account for the unbalanced networks in the future work.

References

[1] P. Hallberg, *et al*. "Active Distribution System Management-A Key Tool For The Smooth Integration Of Distributed Generation," Eurelectric, Brussels, Belgium, Feb. 2013.

[2] N. Mahmud and A. Zahedi, "Review of control strategies for voltage regulation of the smart distribution network with high penetration of renewable distributed generation," *Renew. Sustain. Energy Rev.*, vol. pp. 582-595, 2016.

[3] Y. P. Agalgaonkar, B. C. Pal, and R. A. Jabr, "Distribution voltage control considering the impact of PV generation on tap changers and autonomous regulators," *IEEE Trans. Power Syst.*, vol. 29, no. 1, pp. 182-192, Jan. 2014.

[4] M. H. J. Bollen and A. Sannino, "Voltage control with inverter-based distributed generation," *IEEE Trans. Power Delivery*, vol. 20, no. 1, pp. 519-520, Jan. 2005.

[5] V. Calderaro, G. Conio, V. Galdi, G. Massa, and A. Piccolo, "Optimal decentralized voltage control for distribution systems with inverter-based distributed generators," *IEEE Trans. Power Syst.*, vol. 29, no. 1, pp. 230-241, Jan. 2014.

[6] G. Cavraro, R. Carli, "Local and distributed voltage control algorithms in distribution network," *IEEE Trans. Power Syst.*, vol. 33, no. 2, pp. 1420-1430, Mar. 2018.

[7] K. E. Antoniadou-Plytaria, I. N. Kouveliotis-Lysikatos, P. S. Georgilakis, and N. D. Hatziargyriou, "Distributed and decentralized voltagecontrol of smart distribution networks: Models, methods, and future research," *IEEE Trans. Smart Grid*, vol. 8, no. 6, pp. 2999-3008, Nov. 2017.

[8] S. Liew and G. Strbac, "Maximising penetration of wind generation in existing distribution networks," *IEE Proc. Gener. Transm. Distrib.*., vol. 149, no. 3, pp. 256-262, May 2002.

[9] Q. Zhou and J. W. Bialek, "Generation curtailment to manage voltage constraints in distribution networks," *IET Gener. Transm. Distrib.*, vol. 1, pp. 4929-498, 2007.

[10] S. Weckx, C. Gonzalez, and J. Driesen, "Combined central and local active and reactive power control of PV inverters," *IEEE Trans. Sustain. Energy*, vol. 5, no. 3, pp. 776-784, Jul. 2014.

[11] V. Calderaro, V. Galdi, F. Lamberti, and A. Piccolo, "A smart strategy for voltage control ancillary service in distribution networks," *IEEE Trans. Power Syst.*, vol. 30, no. 1, pp. 494-502, Jan. 2015.

[12] A. Kulmala, S. Repo, and P. Jarventausta, "Coordinated voltage control in distribution networks including several distributed energy resources," *IEEE Trans. Smart Grid*, vol. 5, no. 4, pp. 2010-2020, Jul. 2014.

[13] P. Li, H. Ji, C. Wang, J. Zhao, G. Song, F. Ding, and J. Wu, "A coordinated control method of voltage and reactive power for active distribution networks based on soft open point," *IEEE Trans. Sustain. Energy*, vol. 8, no. 4, Oct. 2017.

[14] Y. J. Kim, J. L. Kirtley, and L. K. Norford, "Reactive power ancillary service of synchronous DGs in coordination with voltage control devices," *IEEE Trans. Smart Grid*, vol. 8, no. 2, pp. 515-527, Mar. 2017.

[15] K. Christakou, D.-C. Tomozei, M. Bahramipanah,J.-Y. Le Boudec, and M. Paolone, "GECN: Primary voltage control for active distribution networks via real-time demand-response," *IEEE Trans. on Smart Grid*, vol. 5, no. 2, pp. 622-631, Mar. 2014.

[16] K. Christakou, D.-C. Tomozei, M. Bahramipanah,J.-Y. Le Boudec, and M. Paolone, "Primary voltage control in active distribution networks via broadcast signals: The case of distributed storage," *IEEE Trans. Smart Grid*, vol. 5, no. 5, pp. 2314-2325, Sep. 2014.

[17] V. Zamani, A. Cortés, J. Kleissl, and S. Martínez, "Integration of PV generation and storage on power distribution systems using MPC," in *Proc. IEEE Power Energy Soc. Gen. Meeting*, 2015, pp. 1-5.

[18] G. Cavraro, T. Caldognetto, R. Carli and P. Tenti, "A master/slave control of distributed energy resources in low-voltage microgrids," 2016 European Control Conference (ECC), Aalborg, 2016, pp. 1507-1512.

[19] T. Caldognetto, S. Buso, P. Tenti and D. I. Brandao, "Power-Based Control of Low-Voltage Microgrids," *IEEE J. Emerg. Sel. Top. Power Electron.*, vol. 3, no. 4, pp. 1056-1066, Dec. 2015.

[20] L. Cheng, Y. Chang, R. Huang, "Mitigating voltage problem in distribution system with distributed solar generation using electric vehicles," *IEEE Trans. Sustain. Energy*, vol. 6, no. 4, pp. 1475-1484. Oct. 2015.

[21] B. A. Robbins, C. N. Hadjicostis, and A. D. Domínguez-García, "A two-stage distributed architecture for voltage control in power distribution systems," *IEEE Trans. Power Syst.*, vol. 28, no. 2, pp. 1470-1482, May 2012.

[22] M. Zeraati, M. E. Golshan, and J. M. Guerrero, "A consensus-based cooperative control of PEV battery and PV active Power curtailment for voltage Regulation in distribution networks," *IEEE Trans. Smart Grid*, in press.

[23] P. Šulc, S. Backhaus, and M. Chertkov, "Optimal distributed control of reactive power via the alternating direction method of multipliers," *IEEE Trans. Energy Convers.*, vol. 29, no. 4, pp. 968-977, Dec. 2014.

[24] K. Christakou, J. LeBoudec, M. Paolone, and D.-C. Tomozei, "Efficient computation of sensitivity coefficients of node voltages and line currents in unbalanced radial electrical distribution networks," *IEEE Trans. Smart Grid*, vol. 4, no. 2, pp. 741-750, Jun. 2013.

[25] P. Lagonotte, J. C. Sabonnadiere, J. Y. Leost, and J. P. Paul, "Structural analysis of the electrical system: Application to secondary voltage control in France," *IEEE Trans. Power Syst.*, vol. 4, no. 2, pp. 479-486, May 1989.

[26] H. Sun, Q. Guo, B. Zhang, W. Wu, and B. Wang, "An adaptive zone division-based automatic voltage control system with applications in China," *IEEE Trans. Power Syst.*, vol. 28, no. 2, pp. 1816-1828, May 2013.

[27] V. Alimisis, P. C. Taylor, "Zoning Evaluation for Improved Coordinated Automatic Voltage Control," *IEEE Trans. Power Syst.*, vol. 30, no. 5, pp. 2736-2746, Sep. 2015.

[28] Y. Guo, H. Gao, Q. Wu, H. Zhao, J. Østergaard, and M. Shahidehpour, "Enhanced voltage control of VSC-HVDC connected offshore wind farms based on Model Predictive Control," *IEEE Trans. Sustain. Energy*, vol. 9, no. 1, pp. 474-487, Jan. 2018.